

X-ray diffraction as a highly selective and sensitive tool for the identification of Mg-rich carbonate phases in terms of the limestone with magnesium practical application

*Katarzyna STANIENDA-PILECKI¹**

Authors' affiliations and addresses:

¹ Silesian University of Technology, Faculty of Mining, Safety Engineering and Industrial Automation, Department of Applied Geology Akademicka 2 Street, 44-100 Gliwice, Poland e-mail: Katarzyna.Stanienda-Pilecki@polsl.pl

*Correspondence:

Katarzyna Stanienda-Pilecki, Silesian University of Technology, Faculty of Mining, Safety Engineering and Industrial Automation, Department of Applied Geology Akademicka 2 Street, 44-100 Gliwice, Poland tel.: +48 322371026 e-mail: Katarzyna.Stanienda-Pilecki@polsl.pl

How to cite this article:

Stanienda-Pilecki, K. (2023). X-ray diffraction as a highly selective and sensitive tool for the identification of Mg-rich carbonate phases in terms of the limestone with magnesium practical application. *Acta Montanistica Slovaca*. Volume 28 (2), 358-372

DOI:

<https://doi.org/10.46544/AMS.v28i2.08>

Abstract

This article presents the theory about the usability and effectiveness of X-Ray Diffraction in identifying carbonate phases varied in magnesium content in the practical application of limestone-rich magnesium. Results of research on the Triassic limestone samples using this method are presented there. The samples were taken from the area of Opole Silesia in Poland. It is a Polish part of the Germanic Basin. X-ray diffraction was used to identify the following phases: low-Mg calcite, high-Mg calcite, dolomite, and huntite. Low-Mg calcite dominates in the limestones. In some samples, there is also a lower amount of high-Mg calcite. Moreover, dolomite and huntite were identified. The study results have shown that X-ray diffraction is the perfect method to identify carbonate phases with different magnesium content. Limestone, including carbonates rich in magnesium, can be used as a fertilizer, animal feed additive, sorbent to desulfurize flue gases or material in road building. The research results indicate the possibility of application of the Muschelkalk limestones rich in magnesium from the area of Opole Silesia in different branches of industry. Therefore, it would not be necessary to carry out selective exploitation in a way to avoid the magnesium-rich limestone zones in the deposits.

Keywords

X-ray Diffraction, low-Mg calcite, high-Mg calcite, dolomite, huntite, limestone-rich in Mg application



© 2023 by the authors. Submitted for possible open access publication under the terms and conditions of the Creative Commons Attribution (CC BY) license (<http://creativecommons.org/licenses/by/4.0/>).

Introduction

Biogenic and inorganic rhombohedral carbonate minerals with variable content of CaCO_3 and MgCO_3 occur in a natural form in nature (Morse et al., 2006; Boggs, 2010; Nash et al., 2011; Mackenzie & Andersson, 2013). They were also identified in Triassic limestones of the Polish part of the Germanic Basin (South-West part of Poland – area of the Opole Silesia) (Szulc, 2000; Stanienda, 2008, 2013a,b). These limestones are Lower Muschelkalk (Middle Triassic) sediments. The Muschelkalk profile contains Gogolin Beds (the bottom of the profile), Górażdże Beds, Dziewkowice Beds, and Karchowice Beds (the upper formation of the profile). The formation names are regional. They come from the names of nearby towns. The limestones of these units are built of carbonate phases different in Ca and Mg content. Results of the hitherto conducted studies show that these limestones are mainly built of low-Mg calcite (low magnesium calcite), high-Mg calcite (high magnesium calcite), and dolomite. Moreover, it is possible to observe lesser amounts of huntite, ankerite, and siderite (Stanienda, 2013a,b, 2014, 2016a,b; Stanienda-Pilecki, 2017, 2018, 2021). The Muschelkalk limestones were first investigated as a part of previous projects. These researches were connected with identifying carbonate mineral phases in limestones with the application of different analytical methods and studies of diagenetic processes. X-ray diffraction was then one of the methods used during the research (Stanienda, 2013a,b, 2016a,b; Stanienda-Pilecki, 2017, 2018, 2021). However, the application of this method, its usefulness, effectiveness, and significance were not analyzed in detail in terms of the identification of carbonate phases varied in magnesium content, especially phases with Mg substitution. The amount of magnesium, in particular, Mg substitution, will affect the crystal structure of the carbonate mineral and, thus, the type and intensity of individual diffraction lines. Therefore, it was decided to elaborate on this problem in the present article.

The X-ray diffraction like FTIR spectroscopy and microprobe measurements allows identifying carbonates characterized by variable content of Ca and Mg: low-Mg calcite- CaCO_3 (space group $R\bar{3}c$), high-Mg calcite CaMgCO_3 (space group $R\bar{3}c$), proto-dolomite $\text{Ca}_{0.5}\text{Mg}_{0.5}\text{CO}_3$ (space group $R\bar{3}c$), ordered dolomite $\text{Ca}_{0.5}\text{Mg}_{0.5}\text{CO}_3$ (space group $R\bar{3}$), huntite $\text{Ca}_{0.25}\text{Mg}_{0.75}\text{CO}_3$ (space group $R32$) and magnesite MgCO_3 (space group $R\bar{3}c$) (Althoff, 1977; Böttcher et al., 1997; Yavuz et al., 2006; Ji et al., 2009; Deelman, 2011; Stanienda, 2013a,b; Stanienda-Pilecki, 2019). The significance of this method is related to the crystal structure analysis during the measurement. The parameters of the carbonate phase unit cell are important (Dollase & Reeder, 1986; Chichagov et al., 2001; Zhang et al., 2010). Magnesium found in carbonate minerals usually comes from seawater. Sometimes it could come from fresh waters. The individual magnesium-containing carbonate phases are characterized by a different content of this element and thus by different parameters of the unit cell and crystal structure (Dollase & Reeder, 1986; Chichagov et al., 2001). High-Mg calcite is an unstable carbonate phase with respect to low-Mg calcite. It may lose its magnesium in time and alter to low-Mg calcite (Kralj et al., 2004; Morse et al., 2006; Boggs, 2010; Mackenzie & Andersson, 2013). Then its crystal structure and parameters of the unit cell could be changed. In X-ray diffraction patterns, the change in the type and intensity of diffraction lines is observed then. If high-Mg calcite is exposed to magnesium-rich pore waters, it can gain additional Mg and be replaced by dolomite (Boggs, 2010). Dolomite and huntite are stable carbonate phases because Mg does not substitute Ca in these phases, and the Mg content is constant (Dollase & Reeder, 1986; Ji et al., 2009; Deelman, 2011). Typical dolomite, stoichiometric in its chemical composition, contains 46.13% of MgCO_3 . It is formed during advanced stages of diagenesis in a water environment rich in magnesium (Morse et al., 2006). Huntite has an increased content of magnesium, from 20-21% of Mg (69-71% MgCO_3) (Dollase & Reeder 1986; Deelman, 2011).

Limestones are usually used in different branches of industry. In the lime industry and usually for flue gas desulphurization in power plants, "pure" limestone is used (Ikavalko et al., 1995; Stanienda, 2013a; Stanienda-Pilecki, 2017, 2021). This type of material characterizes by a low content of admixtures of elements such as Mg, Fe, Si, and Al. Usually, for desulfurization of flue gases, limestone with content of $\text{MgO} < 2\%$ is used. However, the presence of magnesium in carbonate sorbent could make a desulfurization process more effective, especially the application of a sorbent with Mg in dry desulfurization, mainly in the modern method using a Fluidized Bed Reactor (Stanienda-Pilecki, 2017, 2021). Limestones are also applied as a fertilizer (Panhwar et al., 2020; Bide et al., 2021), animal feed additive (Crawford et al., 2008; Cruz et al., 2017), in the building industry, including cement production and in road building (Harris & Chowdhury, 2007; Skorseth et al., 2015).

The aim of this article is to show the effectiveness and importance of X-ray diffraction in the identification of Middle Triassic sediments in the carbonate phases, which include different content of MgCO_3 in the term of the possibility of the practical application of limestones varying in terms of magnesium content. Four phases were determined in analyzed carbonate rocks – low-Mg calcite CaCO_3 , high-Mg calcite $(\text{Ca}_{1-n}, \text{Mg}_n)\text{CO}_3$, dolomite $\text{CaMg}(\text{CO}_3)_2$ and huntite $\text{CaMg}_3[\text{CO}_3]_4$. The article is important because the research results show that substituting Ca^{2+} with Mg^{2+} in the carbonate phases lattices leads to a continuous decrease in the values of their diffraction lines. For this reason, X-ray diffraction allows for the precise identification of carbonate phases with different magnesium content. Because of that, X-ray diffraction is considered to be one of the most useful and effective methods for identifying carbonate phases with variable content of Mg. The results of the study show

that limestones built of mineral phases with variable magnesium content can be used in selected branches of the industry, depending on the amount of Mg. Therefore, it is very important to determine both the type of magnesium carbonate phases and the amount of magnesium in the limestones.

Materials and Method

Materials

The X-ray diffraction was applied to investigate in total 18 samples: 4 from Gogolin Beds – G1, G2, and G6, collected in Gogolin Quarry, LD 11, collected in Górażdże Quarry, 4 samples from Górażdże Beds – SA5 from Saint Anne Mountain area, W1 and W7 collected in Wysoka Quarry, SO25 from Strzelce Opolskie Quarry, 4 samples of Dziewkowice (Terebratula) Beds – S2 and S7 from Szymiszów Quarry, SA12 from Saint Anne Mountain area and SO28 from Strzelce Opolskie Quarry, and 6 samples from Karchowice Beds – SO14 and SO17 collected in Strzelce Opolskie Quarry, T7, T15, T22 and T62, from Tarnów Opolski Quarry (Fig. 1). The samples were collected during leading previous projects connected with study of limestone mineral composition, especially carbonate phases with different Mg content and diagenetic processes of Muschelkalk limestones from the area of the Opole Silesia (South-West part of Poland) (Szulc, 2002; Stanienda, 2008, 2013a,b, 2014, 2016a,b; Stanienda-Pilecki, 2017, 2018, 2021).

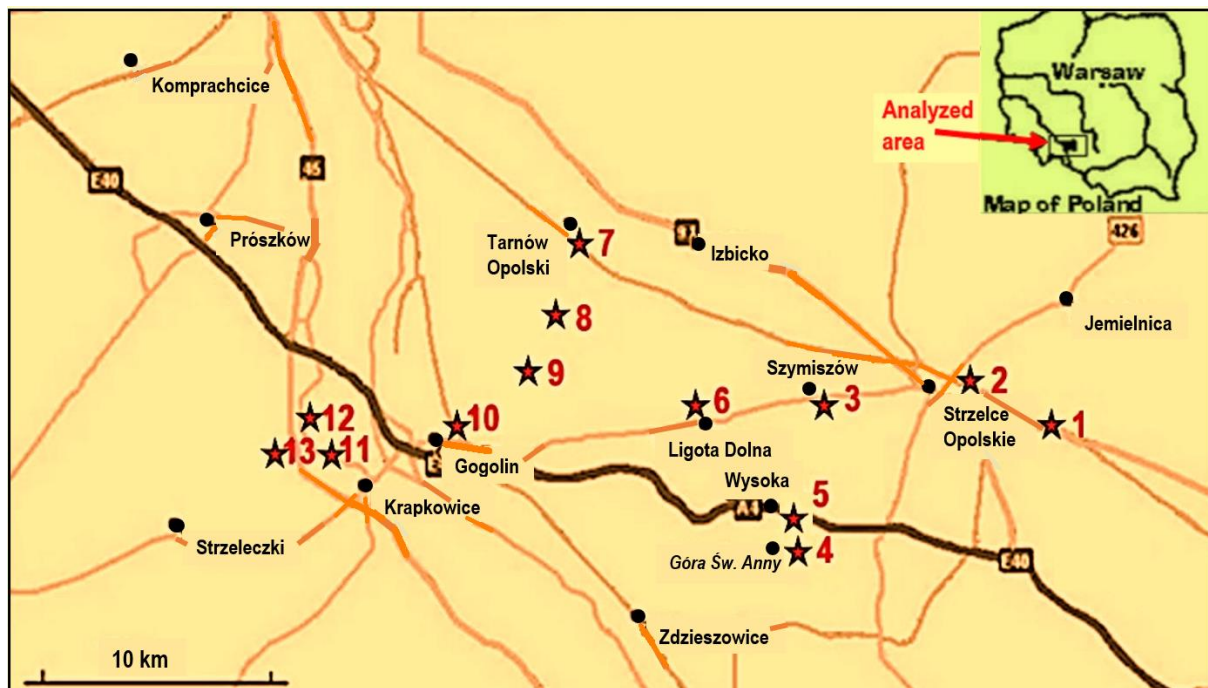


Fig. 1. Location of the investigated area.

1- Błotnica Strzelecka; 2- Dziewkowice; 3- Szymiszów; 4- Saint Anne Mountain; 5- Wysoka; 6- Ligota Dolna and Kamienna; 7- Tarnów Opolski; 8- Kamień Śląski; 9- Górażdże and Kamionek; 10- Gogolin; 11- Malnia; 12- Chorula; 13- Rogów Opolski

★ areas of sampling

Method

The X-ray diffraction analysis of samples G1, G2, G6, LD11, SA5, W, W7, SO25, S2, S7, SA12, SO1, SO14, and SO17 was carried out at the Department of Applied Geology in Gliwice, using the diffractometer HZG4, applying a copper lamp with a nickel screen and the following analysis conditions: voltage 35kV, intensity 18mA. The method of reflective light was used here. X-ray diffraction of samples T7, T15, T22, and T62 was carried out using an X-ray Diffractometer XRD 7 made by Seifert-FPM. Measurements were executed with a range of d-spacing (Å) from 0.8563 nm to 0.0953 nm. The results of the research were compared and analyzed according to data presented in the MINCRYST database (Tab. 1) (Chichagov et al., 2001).

Tab. 1. Typical diffraction lines with their intensities of carbonate phases different in Mg content (Chichagov et al., 2001)

Mineral	d_{hkl} – index of the lattice intervals of exposed parallel lattice planes system (Å) I – the intensity of diffraction lines (in brackets)
low-Mg calcite	3.85478 (16), 3.03555 (100), 2.8435 (2), 2.4948 (13), 2.28463 (28), 2.09443 (19), 1.92739 (8), 1.9124 (21), 1.87532 (29), 1.6258 (3), 1.60409 (11), 1.58689 (1), 1.52524 (9), 1.51777 (3), 1.50937 (5), 1.47317 (2), 1.44037 (12), 1.42175 (5), 1.35677 (1), 1.33897 (3), 1.29666 (5), 1.2474 (1), 1.23525 (2), 1.17979 (3), 1.15378 (7), 1.14232 (4), 1.06144 (1), 1.04721 (5), 1.04479 (6), 1.03526 (3), 1.01185 (7)
high-Mg calcite I	3.83655 (8), 3.02003 (100), 2.82718 (2), 2.48365 (14), 2.27395 (21), 2.08491 (15), 1.91827 (6), 1.9019 (21), 1.86591 (23), 1.61851 (4), 1.59685 (11), 1.57805 (1), 1.51817 (6), 1.51001 (3), 1.50141 (3), 1.46624 (2), 1.43394 (8), 1.41359 (4), 1.35018 (1), 1.33194 (3), 1.29026 (3), 1.24182 (1), 1.22854 (2), 1.1738 (3), 1.14852 (6), 1.13698 (3)
high-Mg calcite II	3.8126 (7), 2.99947 (100), 2.80533 (2), 2.4691 (13), 2.25994 (22), 2.07246 (15), 1.9063 (6), 1.88789 (21), 1.85345 (23), 1.609 (4), 1.58739 (11), 1.56625 (1), 1.50891 (6), 1.49973 (2), 1.49083 (3), 1.45714 (2), 1.42554 (8), 1.40267 (4), 1.34148 (1), 1.3226 (3), 1.28181 (3), 1.23455 (1), 1.21961 (2), 1.16587 (3), 1.14163 (7), 1.12997 (3)
dolomite I Ca(Mg,Ca)[CO ₃] ₂	4.035 (1), 3.69916 (5), 2.89019 (100), 2.67352 (4), 2.54254 (5), 2.407 (11), 2.19487 (28), 2.06714 (3), 2.0175 (14), 1.84958 (5), 1.807 (17), 1.78883 (21), 1.78234 (1), 1.5682 (3), 1.54619 (8), 1.4666 (6), 1.4451 (2), 1.43239 (3), 1.41436 (2), 1.38968 (8), 1.33676 (3), 1.29841 (1), 1.27127 (2), 1.23896 (3), 1.2035 (1), 1.16863 (2), 1.12412 (1), 1.11102 (6), 1.09743 (1)
dolomite II Ca(Mg,Fe)[CO ₃] ₂	3.70285 (9), 2.89464 (100), 2.6799 (2), 2.54694 (2), 2.4085 (13), 2.19689 (22), 2.06849 (1), 2.01898 (14), 1.85142 (5), 1.81072 (17), 1.79136 (21), 1.56921 (3), 1.54726 (9), 1.46786 (7), 1.44732 (3), 1.43492 (3), 1.41573 (1), 1.39055 (8), 1.33995 (3), 1.29995 (1), 1.27347 (2)
dolomite III CaMg[CO ₃] ₂	4.02752 (1), 3.69243 (4), 2.88515 (100), 2.66917 (4), 2.53817 (4), 2.4025 (11), 2.19085 (28), 2.06329 (3), 2.01376 (15), 1.84622 (5), 1.80398 (19), 1.78568 (23), 1.77944 (1), 1.56528 (4), 1.54332 (10), 1.4639 (7), 1.44258 (3), 1.42994 (4), 1.41178 (3), 1.38708 (9), 1.33458 (4), 1.29608 (2), 1.26909 (3), 1.23675 (3), 1.20125 (1), 1.16666 (2), 1.12215 (2), 1.10897 (8), 1.09543 (2)
dolomite IV at 3 GPa+1400°K CaMg[CO ₃] ₂	3.70803 (6), 2.91173 (100), 2.71502 (5), 2.56608 (3), 2.40445 (10), 2.19855 (30), 2.06551 (3), 2.01743 (15), 1.85402 (5), 1.82931 (18), 1.81001 (10), 1.80003 (25), 1.56678 (3), 1.54549 (9), 1.46823 (7), 1.45586 (3), 1.44608 (4), 1.41733 (2), 1.38821 (10), 1.35751 (4), 1.30383 (2), 1.28304 (3), 1.24537 (4), 1.20222 (1), 1.18212 (2), 1.14362 (1), 1.13196 (2), 1.11123 (7), 1.09927 (2)
huntite	5.6693 (1), 4.75135 (1), 3.64157 (2), 2.8903 (18), 2.83465 (100), 2.74319 (2), 2.60707 (8), 2.43434 (9), 2.37568 (10), 2.28561 (5), 2.19108 (7), 1.98971 (7), 1.97127 (23), 1.90234 (1), 1.88977 (1), 1.83528 (3), 1.82078 (2), 1.79584 (3), 1.76605 (15), 1.75597 (14), 1.70022 (3), 1.58378 (9), 1.52538 (2), 1.51702 (1), 1.48493 (5), 1.47893 (4), 1.45237 (2), 1.44515 (2), 1.41732 (2), 1.39748 (2), 1.38261 (1), 1.3716 (2), 1.35359 (1), 1.31779 (3), 1.30353 (4), 1.27858 (1), 1.25919 (1), 1.24521 (1), 1.23915 (2), 1.21717 (1), 1.16259 (1), 1.1428 (1), 1.12588 (3)
magnesite MgCO ₃	2.74089 (100), 2.50215 (13), 2.3164 (6), 2.10212 (51), 1.93805 (14), 1.7692 (5), 1.69982 (44), 1.50876 (5), 1.48641 (8), 1.40601 (7), 1.37045 (2), 1.35364 (11), 1.33737 (15), 1.25108 (5), 1.23819 (2), 1.20197 (2), 1.17948 (4), 1.1582 (1), 1.12837 (1), 1.10078 (1)
ankerite CaFe[CO ₃] ₂	5.389 (1), 3.71499 (12), 2.90657 (100), 2.6945 (1), 2.415 (14), 2.20383 (21), 2.02478 (16), 1.8575 (7), 1.81964 (19), 1.79839 (25), 1.57348 (3), 1.55159 (12), 1.50798 (1), 1.47235 (8), 1.45328 (3), 1.44133 (3), 1.4203 (2), 1.3943 (9), 1.34725 (4), 1.3046 (1), 1.2791 (3), 1.24521 (4), 1.2075 (1), 1.17655 (3), 1.14836 (1), 1.13034 (3), 1.1151 (7), 1.10191 (3)

Results

Minerals of Gogolin Limestones

In total, 4 samples: G1, G2, G6, and LD11 (Tab. 2) were investigated using X-ray spectrometry (Stanienda, 2008, 2013a,b, 2014, 2016a; Stanienda-Pilecki 2018).

The diffraction patterns of samples G1 and G2 were presented in Figures 2 and 3. The study results show that low-Mg calcite dominates in the analyzed samples (Tab. 2, Fig. 2, Fig. 3). Moreover high-Mg calcite, dolomite, and huntite were identified. In the G1 sample, the dolomite was identified based on four diffraction lines but of low intensity, and in the G2 sample, based on one diffraction line, however, the one with the highest intensity (100). Therefore it should be assumed that dolomite is probably present in these samples. Huntite in these samples was identified based on only one diffraction line but one of the highest intensity (100). Therefore it should also be assumed that huntite-like dolomite is probably present in these samples. In samples G6 and LD11, low-Mg calcite dominates (Tab. 2). Moreover, in these samples, huntite was determined based on only one diffraction line but that of the highest intensity. Ankerite was identified in one sample – LD11. Apart from the carbonate minerals, quartz was identified (in samples G2, G6, LD11) and illite (in sample LD11).

Tab. 2. Results of X-Ray Diffraction of limestones from Gogolin Beds

Sample	Mineral	d_{hkl} – index of the lattice intervals of exposed parallel lattice planes system (Å) <i>I</i> – the intensity of diffraction lines (in brackets)
G1 (Fig. 2)	low-Mg calcite	3.8638 (16), 3.0305 (100), 2.8334 (2), 2.4913 (13), 2.0902 (17), 1.9221 (8), 1.8719 (29), 1.6235 (3), 1.6015 (11), 1.5222 (9), 1.5166 (3), 1.5077 (5), 1.5022 (2), 1.4711 (2), 1.4546 (12)
	high-Mg calcite	2.9617 (100), 2.4894 (14), 2.2796 (21), 1.9088 (21), 1.5704 (1), 1.5077 (6), 1.5022 (3), 1.4659 (2)
	dolomite	2.9007 (100), 2.6728 (2), 1.5607 (4), 1.4659 (7)
	huntite	3.6304 (2), 2.9007 (18), 2.8334 (100), 1.8920 (1), 1.4711 (4)
	quartz	4.2369 (19), 3.3300 (100), 2.2796 (7)
	illite	5.0636 (37), 4.5028 (100), 4.3818 (25), 3.9571 (9), 3.8837 (27), 3.3796 (48), 3.2065 (65), 3.1240 (31)
G2 (Fig. 3)	low-Mg calcite	3.8472 (16), 3.056 (100), 2.4927 (13), 2.2823 (28), 2.0948 (17), 1.9241 (8), 1.9107 (21), 1.8737 (29), 1.6248 (3), 1.6028 (11), 1.5814 (1), 1.5256 (9), 1.5155 (3), 1.5044 (5), 1.4711 (2)
	high-Mg calcite	2.9474 (100), 2.8378 (2), 2.4630 (14), 2.2415 (21), 1.6196 (4), 1.5814 (11), 1.5155 (6), 1.5044 (3), 2.9007 (100), 2.0279 (14), 1.8193 (17), 1.5667 (3), 3.6304 (2), 2.8378 (100), 2.3660 (10), 1.9857 (7), 1.9714 (23), 1.7925 (3), 1.7558 (14), 1.4891 (5), 1.4711 (4)
	dolomite	2.9007 (100), 2.0279 (14), 1.8193 (17), 1.5667 (3)
	huntite	3.6304 (2), 2.8378 (100), 2.3660 (10), 1.9857 (7), 1.9714 (23), 1.7925 (3), 1.7558 (14), 1.4891 (5), 1.4711 (4)
	quartz	4.2773 (19), 3.3422 (100), 2.4436 (7), 2.1373 (5), 1.9714 (3)
G6 (Stanienda, 2014, 2016a; Stanienda-Pilecki, 2018)	low-Mg calcite	3.8338 (8), 3.0229 (100), 2.4847 (14), 2.2786 (21), 2.0872 (15), 1.9084 (21), 1.9236 (5), 1.5223 (9), 1.8733 (29), 1.6234 (3), 1.6015 (11), 1.5066 (3)
	high-Mg calcite	2.9402 (100), 1.4691 (2)
	huntite	2.8269 (100)
	quartz	3.3326 (100)
LD11 (Stanienda, 2014, 2016a; Stanienda-Pilecki, 2018)	low-Mg calcite	3.8420 (8), 3.0229 (100), 2.4880 (14), 2.2786 (21), 2.0918 (17), 1.9198 (21), 1.9084 (21), 1.8697 (23), 1.6234 (3), 1.6015 (11), 1.5200 (9), 1.4990 (2)
	huntite	2.8356 (100), 1.4871 (5), 1.4733 (4)
	quartz	4.2503 (20), 3.3387 (100)
	illite	4.9552 (20), 4.4615 (50), 3.3886 (100)

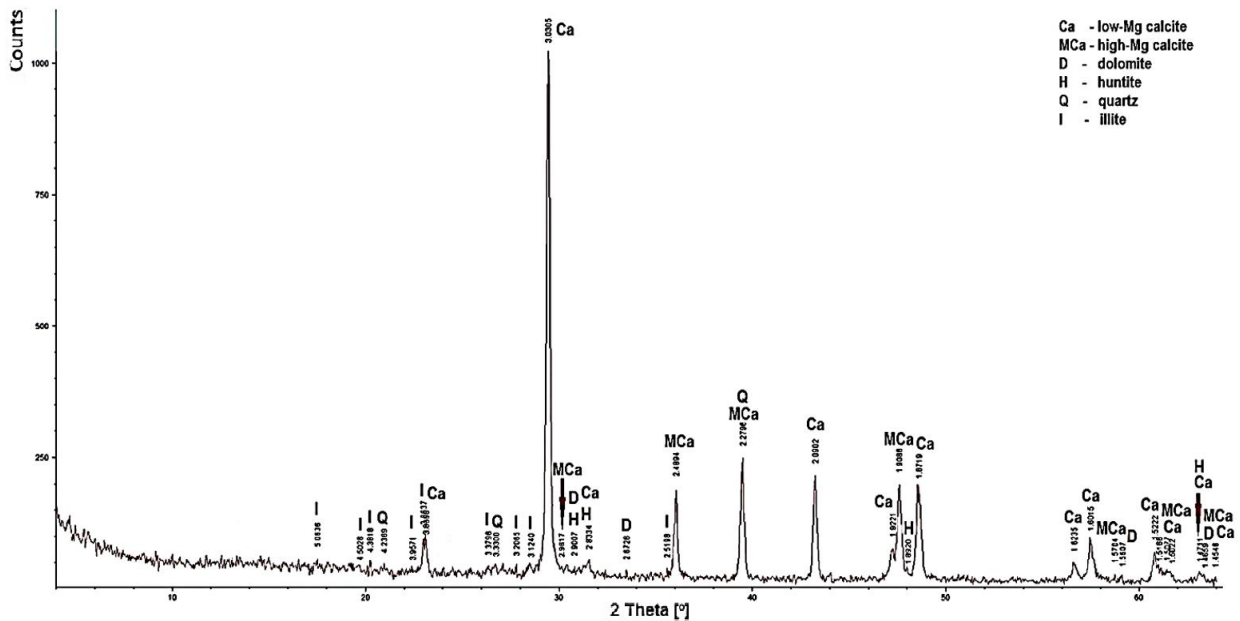


Fig. 2. X-ray diffraction pattern of sample G1 (Gogolin Limestone).

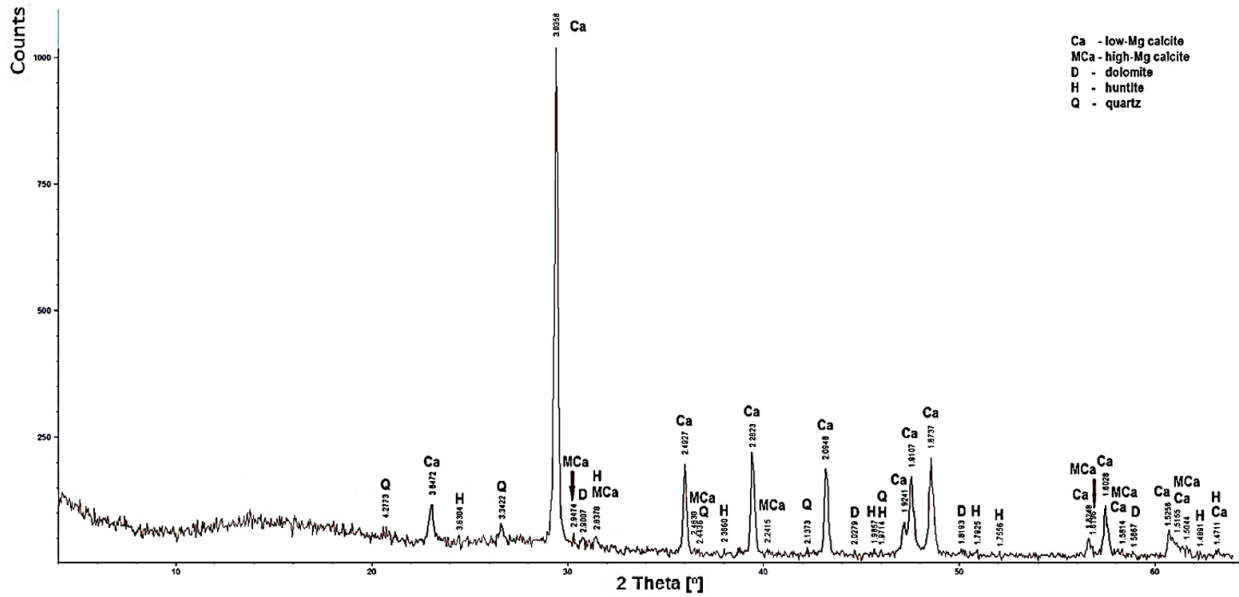


Fig. 3. X-ray diffraction pattern of sample G2 (Gogolin Limestone).

Minerals of Górażdże Limestones

4 samples of Górażdże Beds: SA5, W1, W7, and SO25 (Tab. 3) were investigated using X-ray spectrometry (Stanienda, 2008, 2013a,b, 2014, 2016a,b; Stanienda-Pilecki, 2017).

Figures 4 and 5 present the diffraction patterns of samples SA5 and W1. The results of the study show that in Górażdże limestones also low-Mg calcite dominates. High-Mg calcite was identified in three samples – SA5, W1, and SO25 (Tab. 3, Fig. 4, Fig. 5). This carbonate phase was identified based on two diffraction lines. One of them is the one with the highest intensity. The other carbonate phase – dolomite, was observed in diffraction patterns of samples SA5, W1, and W7 (Tab. 3, Fig. 4, Fig. 5). In the diffraction pattern of sample SA5, only one diffraction line characterized by very low intensity was observed. Therefore it should be assumed that the presence of dolomite in this sample is questionable. In the diffraction pattern of sample W1, dolomite was identified based on only one diffraction line, but the one with the highest intensity (100), and in the diffraction pattern of sample W7, three diffraction lines characterized by low intensity were observed. Therefore it should be assumed that dolomite is probably present in samples W1 and W7. Huntite-like dolomite was also determined in samples SA5, W1, and W7. In samples SA5 and W7, this carbonate phase was identified based on one diffraction line but that of the highest intensity. Therefore should be assumed that huntite-like dolomite is probably present in these samples. In the diffraction pattern of sample W1, one more diffraction line was also observed, characterized by low intensity. Apart from the carbonate minerals, quartz was identified in samples SA5, W7, and SO25.

Tab. 3. Results of X-Ray Diffraction of limestones from Górażdże Beds

Sample	Mineral	d_{hkl} – index of the lattice intervals of exposed parallel lattice planes system (Å) <i>I</i> – the intensity of diffraction lines (in brackets)
SA5 (Fig. 4)	low-Mg calcite	3.8390 (16), 3.0305 (100), 2.8334 (2), 2.4894 (13), 2.2823 (28), 2.0925 (17), 1.9241 (8), 1.9088 (21), 1.8737 (29), 1.6222 (3), 1.6028 (11), 1.5977 (), 1.5246 (9), 1.5144 (3), 1.5044 (5), 1.4723 (2)
	high-Mg calcite	3.0105 (100), 2.8247 (2), 2.2713 (21), 2.0833 (15), 1.9013 (21), 1.8647 (23), 1.6182 (4), 1.5977 (11), 1.4670 (2)
W1 (Fig. 5)	low-Mg calcite	3.8554 (16), 3.0356 (100), 2.8422 (2), 2.4961 (13), 2.2823 (28), 2.0948 (17), 1.9260 (8), 1.9107 (21), 1.8737 (29), 1.6274 (3), 1.6015 (11), 1.5256 (9), 1.5188 (3), 1.5077 (5), 1.4743 (2)
	high-Mg calcite	2.9617 (100), 1.9013 (21), 1.8683 (23), 1.6182 (4), 1.4659 (2)
W7 (Stanienda, 2008, 2016a; Stanienda-Pilecki, 2018)	low-Mg calcite	3.8554 (16), 3.0305 (100), 2.4927 (13), 2.2823 (28), 2.0948 (17), 1.9260 (8), 1.8755 (29), 1.6248 (3), 1.6028 (11), 1.5245 (9), 1.5088 (5), 1.4722 (2)
	dolomite	2.6884 (4), 2.0630 (3), 1.5394 (8)
	huntite	2.8422 (100), 1.9088 (1), 1.5876 (9)
	quartz	3.3361 (100)
SO25 (Stanienda, 2008, 2016a; Stanienda-Pilecki, 2018)	low-Mg calcite	3.8554 (16), 3.0305 (100), 2.4927 (13), 2.2823 (28), 2.0902 (17), 1.9279 (8), 1.8737 (29), 1.6248 (3), 1.6028 (11), 1.5245 (9), 1.5177 (3), 1.5088 (5), 1.4711 (2)
	high-Mg calcite	2.9811 (100), 1.9088 (21), 1.4659 (2)
	quartz	3.3546 (100)

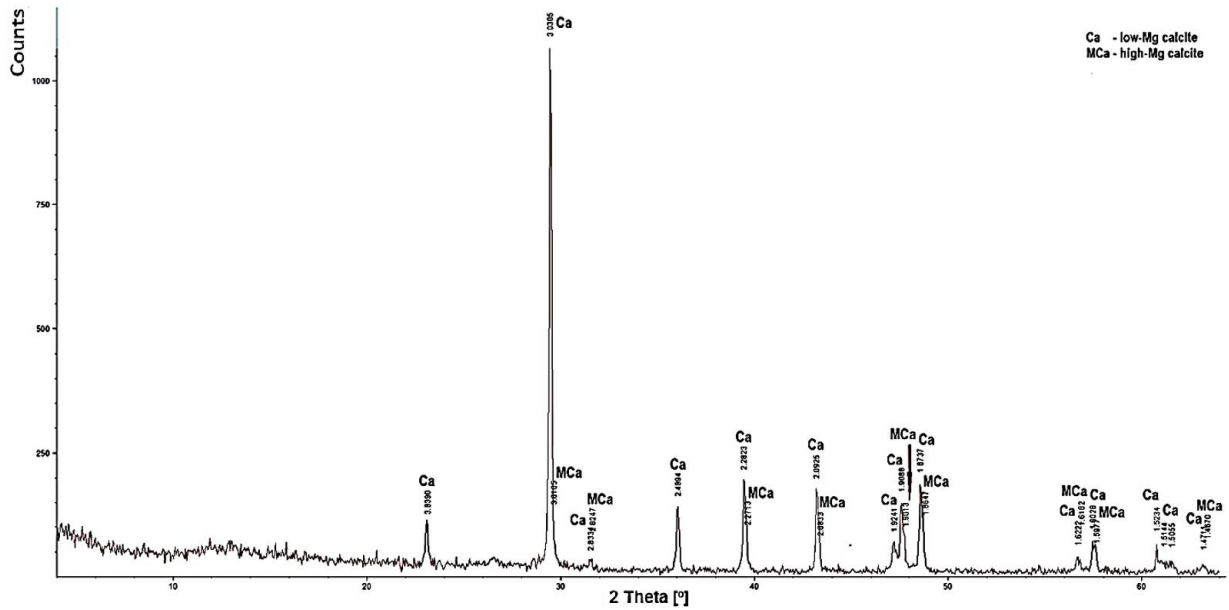


Fig. 4. X-ray diffraction pattern of sample SA5 (Górazdze Limestone).

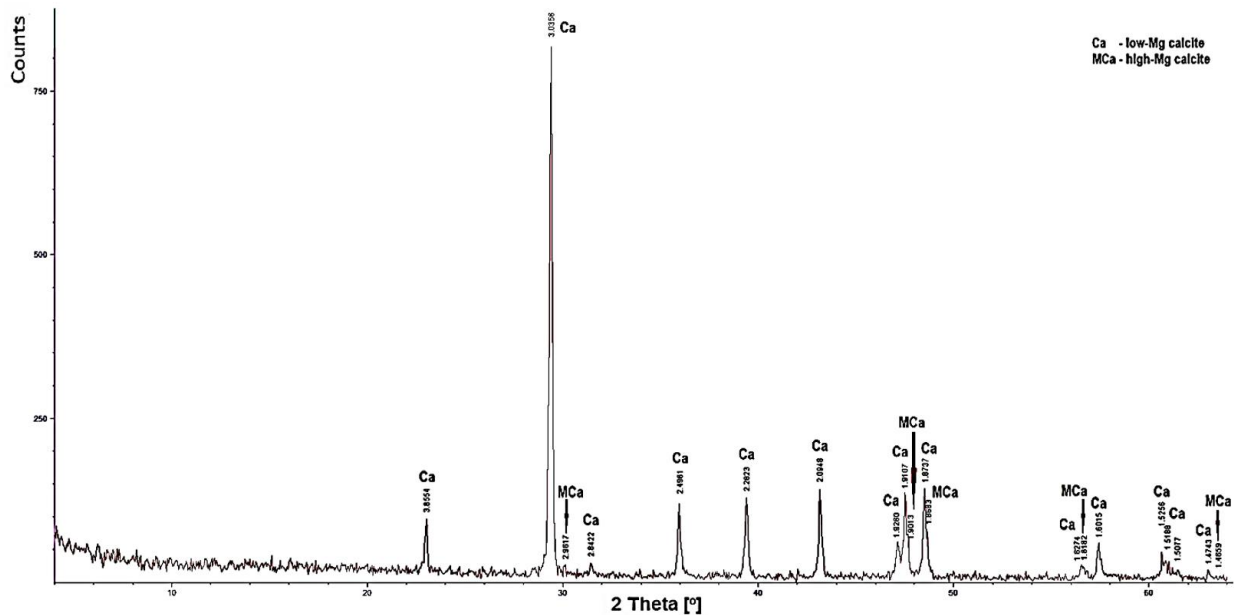


Fig. 5. X-ray diffraction pattern of sample W1 (Górazdze Limestone).

Minerals of Dziejkowice (Terebratula) Limestones

Also, in the case of Dziejkowice limestones, 4 samples in total: S2, S7, SA12, and SO1 (Tab. 4) were investigated using X-ray spectrometry (Stanienda, 2013b, 2016a,b, Stanienda-Pilecki, 2017).

In Figures 6 and 7, the diffraction patterns of samples S2 and S7 were presented. As in previous limestones, these low-Mg calcite dominate (Tab. 4). High-Mg calcite was identified only in samples S2 and S7 on the basis of two diffraction lines. One of them characterizes by the highest intensity. Dolomite was determined in three samples: S2, S7, and SO1 (Tab. 4). In the diffraction patterns of the samples S2 and SO1, five dolomite diffraction lines were observed. But they characterize by low intensities. In all samples, huntite was identified, but on the basis of the one diffraction line with the highest intensity. Therefore should be assumed that huntite is probably present in these samples. Apart from the carbonate minerals, quartz was identified in samples SA12 and SO1.

Tab. 4. Results of X-Ray Diffraction of limestones from Dziewkowiec Beds

Sample	Mineral	d_{hkl} – index of the lattice intervals of exposed parallel lattice planes system (Å) <i>I</i> – the intensity of diffraction lines (in brackets)
S2 (Fig. 6)	low-Mg calcite	3.8554 (16), 3.0305 (100), 2.4927 (13), 2.2851 (28), 2.0925 (17), 1.9260 (8), 1.9107 (21), 1.8755 (29), 1.6248 (3), 1.6053 (11), 1.5245 (9), 1.5155 (3), 1.5055 (5), 1.4732 (2)
	high-Mg calcite	2.9859 (100), 2.0833 (15), 1.9013 (21), 1.8629 (23), 1.5977 (11), 1.5155 (6), 1.5055 (3)
	huntite	2.8378 (100), 2.4468 (9), 2.3541 (10), 1.5716 (9), 1.5245 (2), 1.4732 (4)
	quartz	3.3484 (100), 2.2415 (3), 2.1253 (5), 1.6767 (4), 1.6544 (1), 1.5441 (10),
	feldspar (orthoclase)	3.9484 (17), 3.4050 (51), 3.3057 (100), 2.5581 (41)
S7 (Fig. 7)	low-Mg calcite	3.8554 (16), 3.0305 (100), 2.4927 (13), 2.2823 (28), 2.0925 (17), 1.9260 (8), 1.9107 (21), 1.8755 (29), 1.6261 (3), 1.6040 (11), 1.5256 (9), 1.5088 (5), 1.4722 (2)
	high-Mg calcite	2.9908 (100), 2.4695 (14), 2.2658 (21), 2.0825 (15), 1.9013 (21), 1.8629 (23), 1.6196 (4), 1.5977 (11), 1.5177 (6), 1.4659 (2)
	huntite	3.6015 (2), 2.8378 (100), 2.7162 (2), 2.6123 (8)
	quartz	3.3670 (100), 2.2823 (7), 1.9816 (3), 1.6895 (4)
	feldspar (orthoclase)	3.3057 (100), 3.2122 (77), 2.9427 (7), 2.0193 (14), 1.9455 (3), 1.7203 (1)
SA12 (Stanienda, 2013b; Stanienda-Pilecki, 2017, 2018)	low-Mg calcite	1.9202 (8), 1.5200 (9), 1.5099 (5)
	high-Mg calcite	3.8146 (7), 3.0155 (100), 2.4794 (14), 2.0856 (15), 1.9013 (21), 1.8647 (15), 1.6182 (4), 1.5989 (11), 1.4680 (7)
	huntite	2.8204 (100)
	quartz	3.3239 (100), 2.2255 (3), 1.5595 (10)
SO1 (Stanienda, 2013b; Stanienda-Pilecki, 2017, 2018)	low-Mg calcite	3.8472 (16), 3.0356 (100), 2.4894 (13), 2.2851 (28), 2.0925 (17), 1.9260 (8), 1.9107 (21), 1.8737 (29), 1.6248 (3), 1.6015 (11), 1.5211 (9), 1.5066 (5), 1.4732 (2)
	dolomite	3.7049 (9), 2.0108 (14), 1.5571 (9)
	huntite	2.8334 (100), 1.8244 (2), 1.5876 (9)
	quartz	3.3361 (100), 1.8075 (13)

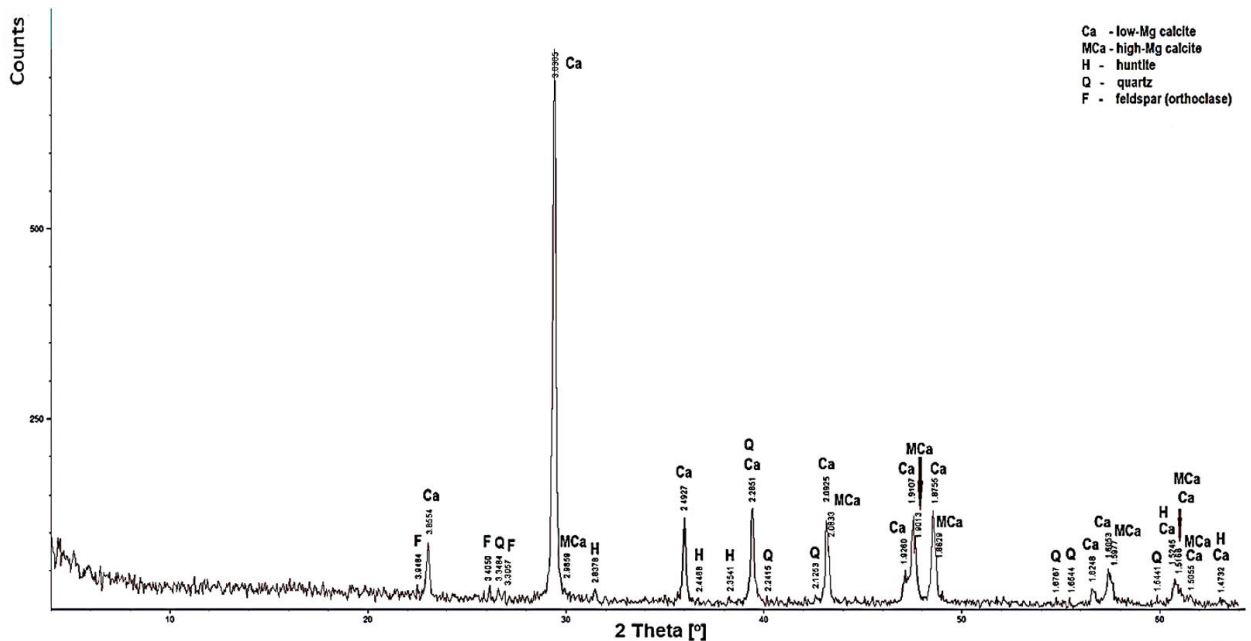


Fig. 6. X-ray diffraction pattern of sample S2 (Dziewkowiec Limestone).

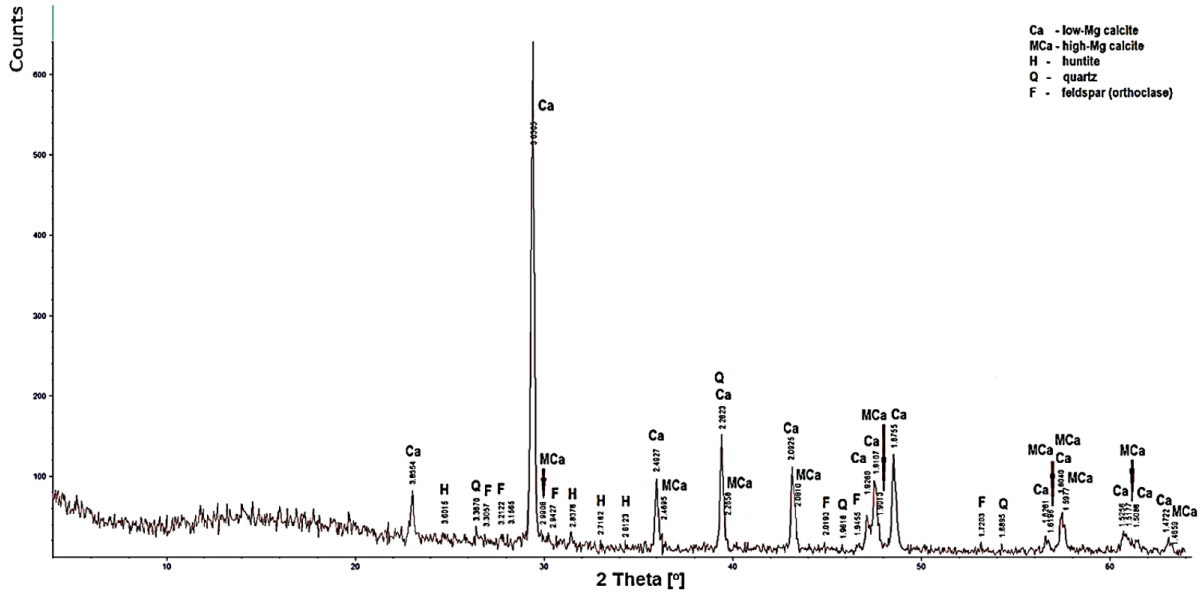


Fig. 7. X-ray diffraction pattern of sample S7 (Dziewkowie Limestone).

Minerals of Karchowice Limestones

In the case of Karchowice Limestones, 6 samples in total: SO14, SO17, T7, T15, T22, and T62 (Tab. 5) were investigated (Stanienda, 2006, 2013a,b, 2016a, Stanienda-Pilecki, 2017, 2018).

The diffraction patterns of two samples – SO14 and T22 were presented in the study (Fig. 8, Fig. 9) (Stanienda, 2013a,b, 2016a, Stanienda-Pilecki, 2017, 2018). The analysis results show that there is also a large amount of dolomite in these limestones apart from low magnesium calcite (Tab. 5). Dolomite was identified based on many diffraction lines. High-Mg calcite was also identified in all samples (Tab. 5). Huntite was observed in the diffraction patterns of two samples: SO14 and SO17. Similarly to previous samples, the huntite of Karchowice limestones was identified based on one diffraction line, the one with the highest intensity. In the diffraction patterns of the samples SO14 and SO17, one diffraction line of ankerite was observed. But it characterizes by very low intensity. Therefore it should be assumed that the presence of ankerite in this sample is questionable. Apart from the carbonate minerals, quartz was identified in samples SO14, SO17, T15, and T22.

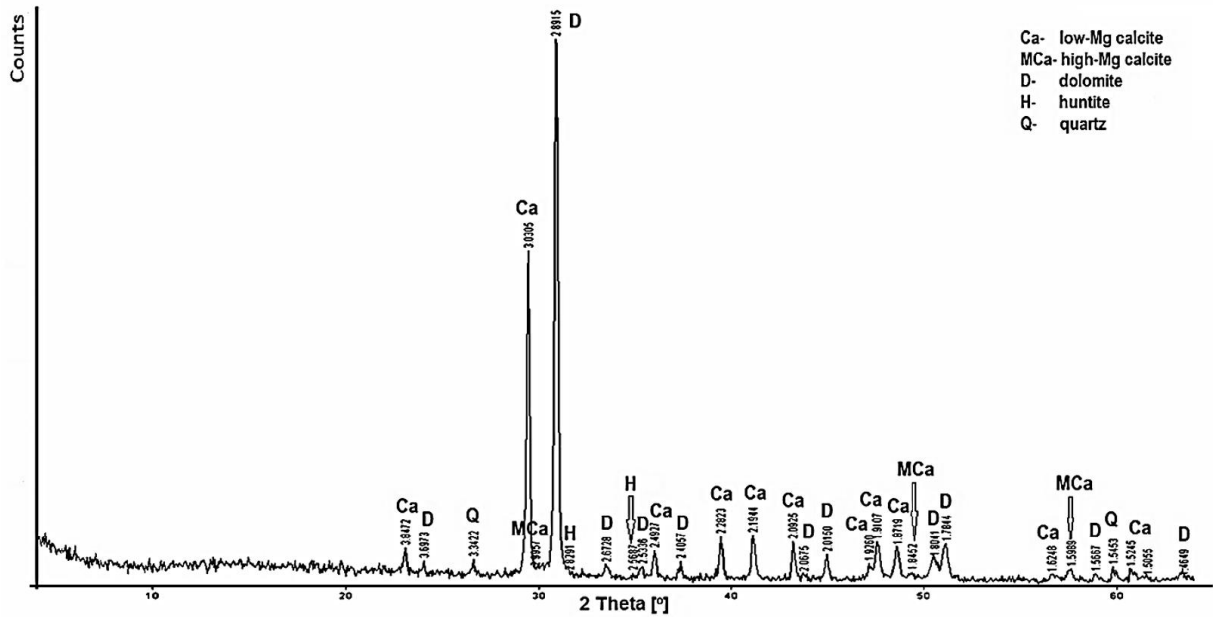


Fig. 8. X-ray diffraction pattern of sample SO14 (Karchowice Limestone) (Stanienda, 2013b, 2016a).

Tab. 5. Results of X-Ray Diffraction of limestones from Karchowice Beds (Stanienda, 2013b, Stanienda-Pilecki, 2017, 2018)

Sample	Mineral	d_{hkl} – index of the lattice intervals of exposed parallel lattice planes system (Å), I – the intensity of diffraction lines (in brackets)
SO14 (Fig. 8)	low-Mg calcite	3.8472 (16), 3.0305 (100), 2.4927 (13), 2.2823 (28), 2.0925 (17), 1.9260 (8), 1.9107 (21), 1.8719 (29), 1.6248 (3), 1.5245 (9), 1.5055 (5)
	high-Mg calcite	2.9957 (100), 1.8452 (23), 1.5989 (11)
	dolomite	3.6973 (5), 2.8915 (100), 2.6728 (4), 2.5336 (5), 2.4057 (11), 2.1944 (28), 2.0675 (3), 2.0150 (14), 1.8041 (17), 1.7844 (1), 1.5667 (3), 1.4649 (6)
	huntite	2.8291 (100), 2.5687 (8)
	quartz	3.3422 (100), 1.5453 (10)
SO17	low-Mg calcite	3.8308 (16), 3.0205 (100), 2.4827 (13), 2.0879 (17), 1.8737 (29)
	high-Mg calcite	2.9908 (100), 2.2768 (15), 1.8629 (15), 1.6002 (4)
	dolomite	2.8779 (100), 2.6690 (4), 2.5406 (3), 2.3964 (7), 2.1893 (28), 2.0129 (14), 1.7975 (17), 1.7827 (1), 1.5655 (3), 1.4639 (6)
	huntite	2.8247 (100), 1.9069 (1)
	ankerite	3.6748 (1)
	quartz	3.3300 (100), 1.5418 (9)
T7	low-Mg calcite	3.865 (16), 3.042 (100), 2.855 (3), 2.495 (12), 2.287 (15), 2.095 (15), 1.928 (5), 1.914 (15), 1.876 (15), 1.627 (4), 1.603 (8), 1.525 (5), 1.513 (4), 1.473 (2), 1.440 (5), 1.338 (2), 1.235 (1), 1.180 (3), 1.154 (3), 1.142 (1), 1.062 (1), 1.046 (3), 1.035 (3)
	high-Mg calcite	2.990 (100), 2.570 (2), 2.260 (15), 1.857 (15), 1.471 (5), 1.423 (3), 1.410 (3), 1.249 (1), 1.193 (3), 1.130 (1), 1.013 (2)
	dolomite	2.895 (100), 2.684 (4), 2.544 (3), 2.410 (7), 2.195 (15), 2.069 (3), 2.027 (10), 1.807 (10), 1.789 (12), 1.470 (2), 1.433 (1), 1.392 (2), 1.296 (2), 1.273 (2), 1.202 (3), 1.125 (1), 1.111 (1), 1.009 (4), 1.0014 (5), 0.9766 (3), 0.9664 (5), 0.9642 (1)
T15	low-Mg calcite	3.870 (12), 3.041 (100), 2.837 (3), 2.496 (12), 2.288 (15), 2.096 (15), 1.925 (5), 1.912 (15), 1.876 (15), 1.626 (4), 1.604 (8), 1.522 (5), 1.513 (4), 1.473 (2), 1.440 (5), 1.234 (1), 1.180 (3), 1.154 (3), 1.143 (1), 1.046 (3), 1.035 (3), 0.9839 (1)
	high-Mg calcite	2.990 (100), 2.570 (2), 1.857 (15), 1.471 (2), 1.422 (3), 1.410 (3), 1.247 (1), 1.190 (3), 1.130 (1), 1.063 (1), 1.042 (1), 1.013 (2)
	dolomite	2.893 (100), 2.020 (10), 1.470 (2), 1.340 (1), 1.298 (2), 1.099 (1), 0.9756 (3), 0.9645 (5)
T22 (Fig. 9)	low-Mg calcite	3.868 (12), 3.039 (100), 2.853 (3), 2.497 (12), 2.286 (15), 2.096 (15), 1.929 (5), 1.914 (15), 1.877 (15), 1.626 (4), 1.604 (8), 1.521 (5), 1.517 (4), 1.441 (5), 1.335 (2), 1.178 (3), 1.153 (3), 1.048 (3)
	high-Mg calcite	2.990 (100), 2.576 (2), 2.260 (15), 1.470 (5), 1.423 (3), 1.249 (1), 1.190 (3), 1.160 (3), 1.130 (1), 1.010 (2)
	dolomite	4.040 (1), 3.715 (4), 3.681 (4), 2.899 (100), 2.680 (4), 2.544 (3), 2.410 (7), 2.198 (15), 2.069 (3), 2.018 (10), 1.800 (10), 1.790 (12), 1.570 (2), 1.546 (4), 1.467 (2), 1.414 (3), 1.388 (15), 1.297 (2), 1.271 (2), 1.240 (5), 1.203 (3), 1.111 (5), 1.069 (1), 1.0098 (4), 1.0018 (5), 0.9754 (3), 0.9661 (1), 0.9547 (1)
	quartz	3.340 (100)
T62	low-Mg calcite	3.862 (12), 3.044 (100), 2.495 (12), 2.285 (15), 2.095 (15), 1.927 (5), 1.911 (15), 1.875 (15), 1.605 (8), 1.525 (5), 1.339 (2), 1.152 (3), 1.042 (3)
	high-Mg calcite	2.990 (100), 2.570 (2), 2.260 (15), 1.854 (15), 1.470 (5), 1.420 (3), 1.410 (3), 1.190 (3), 1.130 (1), 1.013 (2)
	dolomite	3.700 (4), 2.896 (100), 2.680 (4), 2.547 (3), 2.412 (7), 2.197 (15), 2.066 (3), 2.019 (10), 1.808 (10), 1.789 (12), 1.547 (4), 1.468 (2), 1.431 (1), 1.389 (15), 1.296 (2), 1.237 (5), 1.202 (3), 1.168 (1), 1.111 (5), 1.096 (1), 1.068 (1), 1.0094 (4), 1.0015 (5), 0.9744 (3), 0.9627 (5)

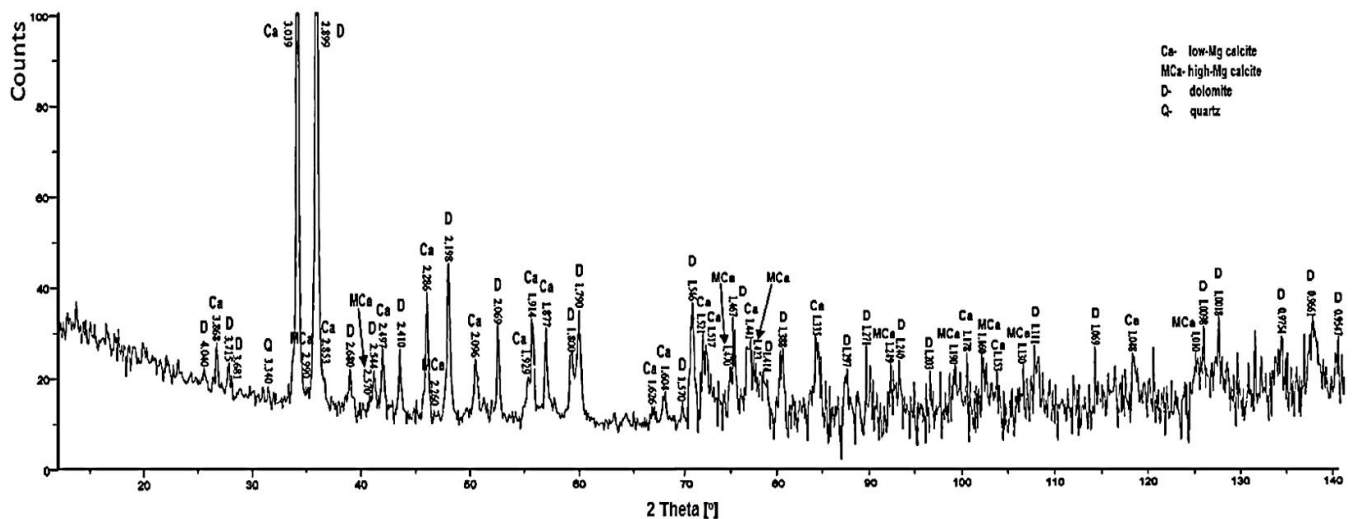


Fig. 9. X-ray diffraction pattern of sample T22 (Karchowice Limestone) (Stanienda, 2016a).

Discussion

Carbonate phases in Triassic limestone

The results of X-ray diffraction indicate that the great variation of carbonate phases occur in limestones of all studied units: Gogolin Beds, Górażdże Beds, Dziewkowice Beds, and also in Karchowice Formation.

Low magnesium calcite – also called "pure" calcite with the chemical formula CaCO_3 dominates in limestones of all formations. This phase was determined on the basis of typical diffraction lines for this carbonate phase (Tab. 1).

High-Mg calcite characterized by general chemical formula $(\text{Ca}_{1-n}\text{Mg}_n[\text{CO}_3])$ was identified in limestone samples of all formations but not in each investigated sample. The chemical formula of high-Mg calcite of Gogolin limestones can be demonstrated as follows: $\text{Ca}_{0.9}\text{Mg}_{0.1}\text{CO}_3$, whereas that of Górażdże limestones is $(\text{Ca}_{0.92-0.90}\text{Mg}_{0.08-0.10})\text{CO}_3$, that of Dziewkowice limestones can be demonstrated as follows: $(\text{Ca}_{0.87-0.74}\text{Mg}_{0.13-0.26})\text{CO}_3$, and that of Karchowice limestones is $(\text{Ca}_{0.85-0.77}\text{Mg}_{0.15-0.23})\text{CO}_3$ (Stanienda, 2013a, 2016a, Stanienda-Pilecki, 2018). The diffraction lines of high-Mg calcite were observed in X-ray diffraction patterns of three Gogolin Limestones: in sample G1 – d_{hkl} : 2.9689 Å (100), 1.5619 Å (1), 1.4660 Å (2), in sample G2 – d_{hkl} : 2.9437 Å (100) and in G6 – d_{hkl} : 2.9402 Å (100), 1.4691 Å (2) (Stanienda, 2014, 2016a). In Górażdże Limestones high-Mg calcite was determined in three samples –: SA5₇ – based on two diffraction lines, with values 2.9593 Å (100), 2.0425 Å (15), W1₇ – based on only one diffraction line, with value 2.9669 Å (100) and SO25₇ – on the basis of three diffraction lines, with values 2.9811 Å (100), 1.9088 Å (21), 1.4659 Å (2). In Dziewkowice Limestones, this phase was identified in three samples: S2 – based on diffraction line 2.9599 Å (100), S7 – based on diffraction line 2.9545 Å (100), and in SA12 – on the basis on diffraction lines: 3.8146 Å (7), 3.0155 Å (100), 2.4794 Å (14), 2.0856 Å (15), 1.9013 Å (21), 1.8647 Å (15), 1.6182 Å (4), 1.5989 Å (11), 1.4680 Å (7) (Stanienda, 2013b; Stanienda-Pilecki, 2018). In Karchowice Limestones diffraction lines of high-Mg calcite were observed in X-ray diffraction patterns of all studied samples: SO14 – diffraction lines: 2.9957 Å (100), 1.8452 Å (23), 1.5989 Å (11)), SO17 – diffraction lines: 2.9908 Å (100), 2.2768 Å (15), 1.8629 Å (15), 1.6002 Å (4), T7 – diffraction lines: 2.990 Å (100), 2.570 Å (2), 2.260 Å (15), 1.857 Å (15), 1.471 Å (5), 1.423 Å (3), 1.410 Å (3), 1.249 Å (1), 1.193 Å (3), 1.130 Å (1), 1.013 Å (2), T15 – diffraction lines: 2.990 Å (100), 2.570 Å (2), 1.857 Å (15), 1.471 Å (2), 1.422 Å (3), 1.410 Å (3), 1.247 Å (1), 1.190 Å (3), 1.130 Å (1), 1.063 Å (1), 1.042 Å (1), 1.013 Å (2), T22 – diffraction lines: 2.990 Å (100), 2.576 Å (2), 2.260 Å (15), 1.470 Å (5), 1.423 Å (3), 1.249 Å (1), 1.190 Å (3), 1.160 Å (3), 1.130 Å (1), 1.010 Å (2) and T62 – diffraction lines: 2.990 Å (100), 2.570 Å (2), 2.260 Å (15), 1.854 Å (15), 1.470 Å (5), 1.420 Å (3), 1.410 Å (3), 1.190 Å (3), 1.130 Å (1), 1.013 Å (2) (Stanienda, 2013b, 2016a, Stanienda-Pilecki, 2018). The investigation results show that substituting Ca^{2+} by Mg^{2+} in the high-Mg calcite lattice leads to continuously decreasing diffraction line values from typical for calcite to characteristic for dolomite (Chichagov et al., 2001). Because the Mg^{2+} presence affects the value of diffraction lines of carbonate phases containing magnesium, the values of the diffraction lines may indicate the amount of Mg which substitutes Ca ions in the structure of high-Mg calcite. Analyzing the diffraction patterns of the tested samples, it is possible to observe a differentiation of the d_{hkl} values with the highest intensity, from 2.9402 Å (the highest amount of Mg substitution) to 3.0155 Å (the lowest amount of Mg substitution). On the diffraction patterns of the samples where high-magnesium calcite was identified, it is also possible to observe a differentiation of the values of the other diffraction lines, depending on the magnesium content. However, the d_{hkl} values are usually lower than these of low magnesium calcite but higher than these of dolomite.

Dolomite ($\text{CaMg}[\text{CO}_3]_2$) was determined in two Gogolin limestone samples: G1 – based on diffraction lines with values: 2.6749 Å (4), 2.0579 Å (3), 1.5716 Å (3) and G2 – based on one diffraction line: 2.8994 Å (100). Dolomite in the G1 sample was identified based on three low-intensity diffraction lines. Therefore, we can only suspect that dolomite is present in this sample. Dolomite probably also occurs in sample G2 because it was identified based on only one diffraction line, but the one with the highest intensity. The dolomite phase was also determined in two samples of Górażdże limestones – W1 and W7. In sample W1, this phase was identified based on two diffraction lines: 2.8964 Å (100), 2.6406 Å (4), and in sample W7 – based on three diffraction lines: 2.6884 Å (4), 2.0630 Å (3), 1.5394 Å (8) characterized by lower intensities. Therefore, dolomite probably occurred in this sample. In Dziewkowice limestones, dolomite was determined in three samples: S2 – based on four diffraction lines: 2.6749 Å (4), 2.0579 Å (3), 1.5619 Å (4), 1.4660 Å (7), S7 – based on three diffraction lines: 2.8954 Å (100), 2.1769 Å (28), 1.4551 Å (6) and SO1 – based on three diffraction lines: 3.7049 Å (9), 2.0108 Å (14), 1.5571 Å (9). In diffraction patterns of samples S2 and SO1, only diffraction lines characterized by lower intensities were observed. Therefore, in this case, it should be assumed that the dolomite is probably present in these samples. In Karchowice Limestones, dolomite was identified in all of the investigated samples: SO14, SO17, T7, T15, T22, and T62. In diffraction pattern of the sample SO14 the following diffraction lines were determined: 3.6973 Å (5), 2.8915 Å (100), 2.6728 Å (4), 2.5336 Å (5), 2.4057 Å (11), 2.1944 Å (28), 2.0675 Å (3), 2.0150 Å (14), 1.8041 Å (17), 1.7844 Å (1), 1.5667 Å (3), 1.4649 Å (6). In diffraction pattern of

SO17 sample the following ones were observed: 2.8779 Å (100), 2.6690 Å (4), 2.5406 Å (3), 2.3964 Å (7), 2.1893 Å (28), 2.0129 Å (14), 1.7975 Å (17), 1.7827 Å (1), 1.5655 Å (3), 1.4639 Å (6). In samples T7, T15, T22, and T62, dolomite was also identified based on numerous diffraction lines (Tab. 5). Based on the results; it can be concluded that dolomite, similarly to low magnesium calcite, dominates in these limestones. The values of dolomite diffraction lines are lower than the values characteristic of high magnesium calcite. This confirms the theory showing that with the increase of the magnesium ions content in the crystal, the value of the diffraction line decreases. The values of the diffraction line with the highest intensity indicate that ordered dolomite is present in studied limestones. According to the principle that the value of the diffraction line decreases with increasing magnesium content in the crystal, the values of proto-dolomite diffraction lines would be higher than those of ordered dolomite. But these values would be lower than those typical for high magnesium calcite.

Huntite ($\text{CaMg}_3[\text{CO}_3]_4$) was determined in three Gogolin limestones— G1, G2, and G6, based on only one diffraction line but the one of the highest intensity and in one sample – LD11 based on the following diffraction lines: 2.8356 Å (100), 1.4871 Å (5), 1.4733 Å (4). The diffraction lines of huntite were observed in diffraction patterns of three samples of the Górażdże limestones – SA5, W1, and W7. In samples SA5 and W1, huntite was identified based on one diffraction line, but the one with the highest intensity. Therefore it can be said that the huntite is probably present in these samples. In the diffraction pattern of sample W7, the following diffraction lines of huntite were observed: 2.8422 Å (100), 1.9088 Å (1), 1.5876 Å (9). Huntite was identified in all of the investigated samples of Dziewkowice limestones – S2, S7, SA12, and SO1. It was determined in sample S2 based on the following diffraction lines: 2.8313 Å (100), 1.5716 Å (9), in sample S7 – based on one diffraction line: 2.8441 Å (100), in sample SA12 – also based on one diffraction line: 2.8204 Å (100) and in sample SO1 – based on three 2.8334 Å (100), 1.8244 Å (2), 1.5876 Å (9). Huntite was identified based on a single diffraction line, but the one of the highest intensity, in the samples S7 and SA12. This indicates the probability of huntite presence in these samples. The diffraction lines of huntite were observed in diffraction patterns of only two of six investigated samples of the Karchowice limestones – SO14 and SO17. In the sample SO14, this carbonate phase was identified based on two diffraction lines: 2.8291 Å (100) and 2.5687 Å (8), and in the sample SO17 – also based on two diffraction lines: 2.8247 Å (100), 1.9069 Å (1). The research results indicate that the values of the highest intensity diffraction line of the huntite are slightly differentiated for some samples. The value of d_{hkl} with the highest intensity (100) varies in range from 2.8204 Å to 2.8422 Å. According to the principle that the value of the diffraction line decreases with increasing magnesium content in the crystal, it can be assumed that the huntite of studied samples is characterized by different Mg content. It is probably related to the varied content of magnesium and calcium ions in the huntite crystal lattice. This type of huntite is probably present in the investigated limestones. The d_{hkl} values lower than typical for huntite, for example, lower than 2.83465 Å for the highest intensity (100), may indicate lowered magnesium content in huntite crystal. Previous studies showed that the Mg content in huntite (14.01-16.18%) is lower corresponding to stoichiometric value: 20-21% Mg (33–34% MgO, 69-71% MgCO_3) but exceeds the stoichiometric value for dolomite (13.12% Mg, 21.86% MgO) (Stanienda, 2013a,b, 2014, 2016a,b; Stanienda-Pilecki, 2017, 2018). The reduction of magnesium ions could be caused by the diagenetic process – dehuntization.

Practical application of limestone with carbonate phases rich in magnesium

Analyzed limestones could be used in different branches of industry – in the lime industry, for flue gas desulphurization in power plants, for preparing a fertilizer, as an animal feed additive, in the building industry, including cement production, and also in road building.

The limestone proper for the lime industry and desulphurization of flue gases in power plants must characterize by a low content of admixtures of elements such as Mg, Fe, Si, and Al. Usually, for lime production and desulfurization of flue gases, limestone with the content of MgO < 2% is used (Ikavalko et al., 1995; Sanders et al., 1995; Stanienda, 2013a,b, 2017; Stanienda-Pilecki, 2021). However, the presence of magnesium in carbonate sorbent used in flue gases desulfurization makes a process more effective, especially the application of a sorbent with Mg in dry desulfurization, mainly in the modern method using Fluidized Bed Reactor (Ikavalko et al., 1995; Stanienda-Pilecki, 2017). However, material with low MgO content, below 2%, is usually applied in these branches of industry. The research results indicate that the limestone of Górażdże Beds and Karchowice Beds will be the best material for the production of lime and sorbent for flue gas desulphurization.

Another application of limestones is their use in the production of fertilizers (Bide et al., 2021; Castro et al., 2016; Panhwar et al., 2020; Bide et al., 2021) and as an additive to animal feed (Mehring et al., 1965; Crawford et al., 2008; Cruz et al., 2017). The results of the study show that the best material for these applications are the limestones rich in magnesium content, so the rocks of Górażdże Beds and of Karchowice Beds, because these limestones include apart from low-Mg calcite and also high-Mg calcite. Some of them also contain dolomite and huntite – magnesium calcium carbonate.

Limestones are also used in the building industry, including cement production and road building (Harris & Chowdhury, 2007; Skorseth et al., 2015). The use of limestone in these branches of the economy does not

require the use of material with low admixtures of elements such as Fe, Mn, Si, and Al. On the contrary, using a material with higher contents is advisable, especially of such elements as Si and Al. Research results indicate that the best material for the building industry, including cement production and road building, are the limestones of Gogolin Beds and of Dziewkowice Beds because these rocks, apart from carbonate minerals, vary in magnesium content also include quartz and aluminosilicate minerals such as illite and potassium feldspar – orthoclase.

Therefore, it is very important to know the type of mineral phases which are present in limestone because it allows us to consider the application of limestone in individual branches of industry.

In conclusion, it can be said that limestone, including low content of carbonate phases rich in magnesium and also a small number of admixtures of minerals including Fe, Mn, Si, and Al elements, could be used for lime production and sorbent for desulfurization of flue gases. Limestones, including increased content of carbonate phases rich in magnesium, could be applied in the production of fertilizers and as an additive to animal feed. Limestones enriched with admixtures, especially Si and Al elements, are the perfect material for the building industry, including cement production and road building.

Conclusions

One of the most important results to come from the investigation of the Triassic limestones of the Polish part of the Germanic Basin using X-ray diffraction is the identification of carbonate phases with different magnesium content. The results of executed analyses indicate the presence of four carbonate phases with magnesium in the Triassic limestones of the Polish part of the Germanic Basin. They are low Mg-calcite, high magnesium calcite, dolomite, and huntite. These carbonate phases were identified in rocks of all formations of the Polish lower Muschelkalk profile. They include: from the bottom Gogolin Beds, next Górażdże Beds, the following are Dziewkowice (Terebratula) Beds and Karchowice Beds, which build the upper part of the analyzed profile.

Low magnesium calcite (Low-Mg calcite), also called "pure" calcite with chemical formula CaCO_3 , dominates in limestones of all formations. This phase was determined based on typical diffraction lines characteristic of this mineral.

High magnesium calcite (High-Mg calcite), characterized by a general chemical formula $\{\text{Ca}_{1-n}\text{Mg}_n[\text{CO}_3]\}$ was identified in limestone samples of all formations but not in each investigated sample. Variation in the values of high magnesium calcite diffraction lines is probably the result of different Mg content in the crystals of this carbonate phase. Dolomite ($\text{CaMg}[\text{CO}_3]_2$) was also determined in limestone samples of all formations but not in each investigated sample. The values of the diffraction line with the highest intensity indicate that probably ordered dolomite is present in studied limestones. Huntite ($\text{CaMg}_3[\text{CO}_3]_4$) is another carbonate phase with magnesium that has been identified in limestone samples of all formations but not in each investigated sample. The d_{hkl} values lower than typical for huntite, for example, lower than 2.83465 Å for intensity 100, may indicate a decrease of magnesium content in huntite crystal. The reduction of Mg ions is probably the effect of the dehuntization process.

Research results indicate that along with the content of magnesium ions in the crystal, the values of diffraction lines decrease. Thus, the highest values of diffraction lines have low-magnesium calcite and the lower, respectively: high-magnesium calcite, dolomite, and huntite. Therefore, X-ray diffraction could be treated as one of the most appropriate methods for identifying carbonate phases differentiated in magnesium content, including phases with magnesium substitution, because of its usability, effectiveness, and high accuracy.

The study results show that the data obtained because of X-Ray diffraction allows us to determine the directions of limestone application in individual branches of industry. The results indicate that the best material for the production of lime and sorbent for flue gas desulphurization is the limestone of Górażdże Beds and Karchowice Beds. For the production of fertilizers and as an additive to animal feeds, the best are the rocks of Górażdże Beds and these of Karchowice Beds, the limestones rich in magnesium content, which include, apart from low-Mg calcite, also and high-Mg calcite and small amounts of dolomite and huntite. The best material for the building industry, including cement production, and for road building are the limestones of Gogolin Beds, and these of Dziewkowice Beds, which include, apart from carbonate minerals varied in magnesium content, also quartz and aluminosilicate minerals – illite and orthoclase.

References

- Althoff, P. L. (1977) Structural refinements of dolomite and a magnesian calcite and implications for dolomite formation in the marine environment. *American Mineralogist*, 62, 772–783. http://www.minsocam.org/ammin/AM62/AM62_772.pdf

- Bide T., Ander E. L. & Broadley M.R. (2021) A spatial analysis of lime resources and their potential for improving soil magnesium concentrations and pH in grassland areas of England and Wales. *Scientific Reports*, 11, 20420. <https://doi.org/10.1038/s41598-021-98735-w>
- Boggs, S., Jr. (2010) Petrology of sedimentary rocks. Second Edition, Cambridge University Press, pp. 313–457. http://www.minsocam.org/ammin/AM76/AM76_1889.pdf
- Böttcher, M. E., Gehlken, P. L. & Steele, F. D. (1997) Characterization of inorganic and biogenic magnesian calcites by Fourier Transform infrared spectroscopy. *Solid State Ionics*, 101-103, 379–1385. [https://doi.org/10.1016/S0167-2738\(97\)00235-X](https://doi.org/10.1016/S0167-2738(97)00235-X)
- Castro G. S. A., Crusciol C. A. C., da Costa C. H. M., Ferrari Neto J. & Mancuso M. A. C. (2016) Surface application of limestone and calcium-magnesium silicate in a tropical no-tillage system. *J. Soil Sci. Plant Nutr.*, 16, 2. versión On-line ISSN 0718-9516. <http://dx.doi.org/10.4067/S0718-95162016005000034>
- Chichagov, A. V., Varlamov, D. A., Dilanyan, R. A., Dokina, T. N., Drozhzhina, N. A., Samokhvalova, O. L. & Ushakovskaya, T. V. (2001) Information-Calculating System on Crystal Structure Data of Minerals. *Crystallography Reports*, 46(5), 876–879 (Translated from Kristallografiya 46(5), pp. 950–954). <http://database.iem.ac.ru/mincryst/reference.html>
- Crawford G. I., Keeler C. D., Wagner J. J., Krehbiel C. R., Erickson G. E., Crombie M. B. & Nunnery G. A. (2008) Effects of calcium magnesium carbonate and roughage level on feedlot performance, ruminal metabolism, and site and extent of digestion in steers fed high-grain diets. *J. Anim. Sci.*, 86, 2998–3013. doi:10.2527/jas.2007-0070
- Cruz F. L. A., Vieira S. L., Kindlein L., Kipper M., Cemin H. S. & Rauber S. M. (2017) Occurrence of white striping and wooden breast in broilers fed grower and finisher diets with increasing lysine levels. *Poultry Science*, 96, 501–510. <http://dx.doi.org/10.3382/ps/pew310>
- Deelman, J. C. (2011) Magnesite and Huntite. In Low-temperature formation of dolomite and magnesite. (Deelman J.C.) http://www.jcdeelman.demon.nl/dolomite/files/13_Chapter6.pdf
- Dollase, W. A. & Reeder, R. J. (1986) Crystal structure refinement of huntite, $\text{CaMg}_3[\text{CO}_3]_4$, with X ray powder data. *American Mineralogist*, 71, 163–166. <https://pubs.geoscienceworld.org/msa/ammin/article-abstract/71/1-2/163/41794/Crystal-structure-refinement-of-huntite-CaMg3-CO3>
- Harris, J. P. & Chowdhury, A. (2007) Tests to identify poor quality coarse limestone aggregates and acceptable limits for such aggregates in bituminous mixes. Report 0-4523-2, Project 0-4523, Texas Transportation Institute. The Texas A&M University System. <http://tti.tamu.edu/documents/0-4523-2.pdf>
- Ikavalko, E., Laitinen, T., Parkka, M. & Yliruokanen, I. (1995) Intercomparizon of trace-element determination in samples from a Coal Fired Power-Plant. *Int. J Environ Anal Chem.*, 61(3), 207–224. <https://doi.org/10.1080/03067319508027235>
- Ji, J., Ge, Y., Balsam, W., Damuth, J. E. & Chen, J. (2009) Rapid identification of dolomite using a Fourier Transform Infrared Spectrophotometer (FTIR): A fast method for identifying Heinrich events in IODP Site U1308. *Marine Geology*, 258, 60–68. DOI:10.1016/j.margeo.2008.11.007
- Kralj, D., Kontrec, J., Brečević, L., Falini, G. & Nöthig-Laslo, V. (2004) Effect of Inorganic Anions on the Morphology and Structure of Magnesium Calcite- Chemistry. *A European Journal*, 10, 1647–1656. <https://doi.org/10.1002/chem.200305313>
- Mackenzie, F. T. & Andersson, A. J. (2013) The Marine carbon system and ocean acidification during Phanerozoic Time. *Geochemical Perspectives*, 2(1). doi:10.7185/geochempersp.2.1
- Mehring A. L. Jr. & Dewey J. Jr. (1965) Magnesium in Limestones for Laying Chickens. *Poultry Science*, 44, 3, 1, 853–860, <https://doi.org/10.3382/ps.0440853> Get rights and content
- Morse, J. W., Andersson, A. J. & Mackenzie, F. T. (2006) Initial responses of carbonate-rich shelf sediments to rising atmospheric pCO_2 and "ocean acidification": Role of high Mg-calcites. *Geochimica et Cosmochimica Acta*, 70, 5814–5830. doi:10.1016/j.gca.2006.08.017
- Nash, M. C., Troitzsch, U., Opdyke, B. N., Trafford, J. M., Russell, B. D. & Kline, D. I. (2011) First discovery of dolomite and magnesite in living coralline algae and its geobiological implications. *Biogeosciences*, 8, 3331–33340. doi:10.5194/bg-8-3331-2011
- Panhwar Q. A., Naher U. E., Shamshuddin J. & Ismail M. R. (2020) Effects of Biochar and Ground Magnesium Limestone Application, with or without Bio-Fertilizer Addition, on Biochemical Properties of an Acid Sulfate Soil and Rice Yield. *MDPI Agronomy*, 10, 1100; doi:10.3390/agronomy10081100
- Skorseth, K., Reid, R. & Heiberger, K. (2015) Gravel roads construction & maintenance guide. FHWA Publication No.: FHWA-OTS-15-0002. US Department of Transportation. Federal Highway Administration. <https://www.fhwa.dot.gov/construction/pubs/ots15002.pdf>
- Stanienda, K. (2008) Characteristic of carbonate phases in the Triassic limestone of Gogolin and Góraźdże Beds from Ligota Dolna, Saint Anne Mountain and Gogolin. *Scientific Journals of Silesian University of Technology*, Mining 285, 259–269.
- Stanienda, K. (2011) Effects of dolomitization processes in the Triassic limestone of Tarnów Opolski Deposit. Gliwice, Silesian University of Technology Press. ISBN: 978-83-7335-872-0

- Stanienda, K. (2013a) Diagenesis of the Triassic limestone from the Opole Silesia in the aspect of magnesian calcite presence. Gliwice, Silesian University of Technology Press. ISBN: 978-83-7880-071-2
- Stanienda, K. (2013b) Huntite in the Triassic limestones of Opolski Silesia. *Mineral Resources Management*, 9(3), 79–98. DOI 10.2478/gospo-2013-0036
- Stanienda, K. (2014) Mineral phases in carbonate rocks of the Gogolin Beds from the area of Opole Silesia. *Mineral Resources Management*, 30(3), 17–42. DOI 10.2478/gospo-2014-0026
- Stanienda, K. (2016a) Carbonate phases rich in magnesium in the Triassic limestones of the East part of Germanic Basin. *Carbonates and Evaporites*, 31, 387–405. DOI 10.1007/s13146-016-0297-2
- Stanienda, K. (2016b) Mineral phases in carbonate rocks of the Góraźdże Beds from the area of Opole Silesia. *Mineral Resources Management*, 32(3), 67–92. DOI 10.1515/gospo-2016-0023
- Stanienda-Pilecki, K. (2017) Carbonate minerals with magnesium in Triassic Terebratula limestone in the term of limestone with magnesium application as a sorbent in desulfurization of flue gases. *Archives of Mining Sciences*, 62(3), 459–482. DOI 10.1515/amsc-2017-0035
- Stanienda-Pilecki, K. (2018) Magnesium calcite in Muschelkalk limestones of the Polish part of the Germanic Basin. *Carbonates and Evaporites*, 33(4), 801–821. DOI.org/10.1007/s13146-018-0437-y
- Stanienda-Pilecki, K. (2021) The Use of Limestones Built of Carbonate Phases with Increased Mg Content in Processes of Flue Gas Desulfurization. MDPI, *Minerals*, 11, 1044. <https://doi.org/10.3390/min11101044>
- Szulc, J. (2000) Middle Triassic evolution of the Northern Peri-Tethys area is influenced by early opening of the Tethys Ocean. *Annales Societatis Geologorum Poloniae*, 70, 1–48. <https://geojournals.pgi.gov.pl/asgp/article/view/12348/10822>
- Yavuz, F., Kirikoğlu, M. S. & Özden, G. (2006) The occurrence and geochemistry of huntite from Neogene lacustrine sediments of the Yalvaç-Yarıkkaya Basin, Isparta, Turkey. *Neues Jahrbuch Fur Mineralogie-Abhandlungen*, 182(2), 201–212. DOI: 10.1127/0077-7757/2006/0045
- Zhang, F., Xu, H., Konishi, H. & Roden, E. E. (2010) A relationship between d_{104} value and composition in the calcite-disordered dolomite solid-solution series. *American Mineralogist*, 95, 1650–1656. DOI:10.2138/am.2010.3414